Buckling, Postbuckling, and Crippling of Shallow-Curved Composite Plates with Edge Stiffeners

Rocky R. Arnold*
Anamet Laboratories Inc., San Carlos, California
S. Y. Yoo†
Hanyang University, Seoul, Korea
and
J. Mayers‡
Stanford University, Stanford, California

A theoretical/analytical capability for prediction of buckling, postbuckling, and crippling of metal and composite shallow-curved plates is presented. The theoretical model accounts for both geometric and material nonlinearities. The composite material formulation is valid for anisotropic lamina with the fundamental nonlinear behavior described by Ramberg-Osgood lamina and matrix stress-strain relations. Transverse shear effects are also included. Correlations with available conventional metal and composite plate experimental data confirm the accuracy of the present approach.

Nomenclature

A_s = stiffener cross-sectional area
$a_{11}, b_{11}, \ldots$ = arbitrary interlaminar shear coefficients
b = plate width
b_s = stiffener spacing
D = plate bending stiffness
e = prescribed end-shortening per unit length
e_{cr} = end-shortening per unit length at buckling
e_{cr_p} = end-shortening per unit length at buckling for a flat plate
e_i, f_i, g_i = arbitrary displacement coefficients
h, t = laminate thickness
h_{pij} = arbitrary membrane stress coefficients
J_s = stiffener equivalent torsional rigidity
k = kth lamina
L = plate length
m, n = number of half-buckle wavelengths in x,y directions, respectively
N = total number of lamina
N_{cr} = buckling load
R = panel radius
$S_{x_k}^{(0)}, S_{x_k}^{(1)}, \ldots$ = stiffness ratio factors
u, v = membrane displacement functions in x,y directions, respectively
u_k, v_k = median surface in-plane displacements of kth lamina
w = lateral displacement function
x, y, z = plate coordinates (see Fig. 1)
Z = nondimensional curvature parameter, $= (b^2/Rt)\sqrt{1-\nu^2}$
α = parameter defined by Eq. (11)
ρ = distance from plate midsurface to stiffener center of rotation
$\sigma_{x_k}, \sigma_{y_k}$ = median surface extensional stresses of kth lamina in plate coordinates
τ_{xy_k} = median surface shearing stresses of the kth lamina in plate coordinates
τ_{yz_k}, τ_{zx_k} = interlaminar shearing stresses of kth matrix layer

Subscripts

e = linear-elastic materials
p = plastic materials

Introduction

FOR the past 60 years or so, aerospace vehicle structures have been typified by all-metal, thin-walled, sheet-stringer construction primarily of aluminum, and to a much lesser degree, steel and titanium. Such vehicles, with aluminum accounting for as much as 80% of airframe material distribution, have covered a spectrum from subsonic conventional aircraft and helicopters to supersonic transports, military aircraft, and missiles. Even the Space Shuttle, devoid of its external surface thermal protection system, fits the typical definition.

More recently, specifically in the last two decades, interest has centered on nonmetallics for flight vehicle structure. Most attractive have been the advanced composites of resin epoxy reinforced by filaments of either boron, graphite, or aramid (Kevlar) due, mainly, to their potential for creating significant weight savings relative to the metals. Only in serendipitous fashion have significant reductions in vehicle production costs surfaced. The potential for both weight and production cost-savings have been all the more inviting during a period in which fuel costs have risen by about an order of magnitude.

Unfortunately, despite initial appearance in the early 1960s, the advanced composites have seen neither widespread application nor fulfillment of the weight-savings potential and spectacular returns originally forecast in the 1960s.[1,2] With regard to application, most has occurred in secondary structure of commercial and military aircraft and, to an increasing degree, in primary structure of the latter. Only very recently has extensive use of composites been noted in primary structure of a number of advanced helicopter designs. Optimistic projections of composite-material usage

Presented as Paper 85-0769 at the AIAA/ASME/ASCE/AHS 26th Structures, Structural Dynamics and Materials Conference, Orlando, FL, April 15-17, 1985; received July 1, 1986; revision received Jan. 20, 1986.

*Principal Engineer. Member AIAA.
†Associate Professor, Department of Aeronautical Engineering.
‡Professor Emeritus. Associate Fellow AIAA.

in advanced technology transports and military aircraft of the 1990s still provide for significant amounts of aluminum, ranging from a low of 20% (transports) to a high of 50% (military aircraft), and up to as much as 15% each of steel and titanium.[3,4]

The basic concerns regarding widespread application of composites for primary structure continue to focus on cost, confidence, and complexity. These concerns are exacerbated by the absence of a research and development base comparable to that underlying the existing status of aluminum technology in particular and the other structural metals in general, and because, traditionally, either new concepts or research results require several decades to mature to widespread application. In commercial transports, introduction of fleet components has been postponed to the latter 1980s for empennage stabilizers, the 1990s for wings, and the turn of the century for fuselages. Meanwhile, only derivatives of existing designs can be expected as gains in efficiency are sought. NASA-industry attempts to design, fabricate, and test empennage primary structures of advanced composites for commercial aircraft such as the DC-10, L-1011, and 737 have evidenced premature failures during development. And, as a direct result, more widespread attention has been directed to the nonlinear nature of composite stress-strain curves and the susceptibility of composite materials to failure in interlaminar tension and shear.[4] In military aircraft, the derated use of composites in primary structure has kept the requirements for aluminum, titanium, and steel close to previous levels in general.

Overall, the restricted use of composites has precluded achievement of the spectacular returns expected no later than the late 1970's.[5] It should not go unnoticed, also, that continuing metallurgical developments with new aluminum alloys to replace 2024-T3 and 7075-T6 have achieved gains in strength and stiffness on the order of 20%, a density reduction on the order of 10%, and an increased temperature-range tolerance.[3,6] It is of interest that aluminum-lithium material, if available, has been proposed for use in the Boeing 747-300 and the McDonnell Douglas MD-89. Thus, pending the development of metal-matrix composites, tradeoff studies aimed at demonstrating weight savings when substituting epoxy matrix composite materials into baseline aluminum designs are no longer expected to be as optimistic. Furthermore, it cannot be overlooked that introduction of more efficient aluminum alloys requires neither major changes in tooling and manufacturing processes nor the retraining of aircraft maintenance and repair personnel.

Whether the vehicle is fabricated of either metal or composite, or a combination of both, it still retains the same basic structural elements. The nature of stressed-skin construction is such that the typical surface element is normally a shallow-curved plate of rectangular planform bounded on all four edges by stiffening members. The stiffening members, viewed across a number of successive elements, can be either discretely or closely spaced. In the first case, under compressive loading, local buckling of the skin can be expected to occur prior to crippling of the stiffener/effective-skin combination. In the latter case, the closely spaced stiffened plate is designed for local buckling of the skin and stiffeners and general instability of the configuration to occur simultaneously (ultimate load). Although the latter situation is often used in design to create the so-called minimum-weight configuration, a question remains as to whether the "minimum-weight" design can be rated most efficient for the relatively light load intensities found in fuselage structure of transports and helicopters and empennage structures of transports.

Results encompassing a wide variety of boundary conditions exist for estimating the effective width of buckled metal skin acting with the stiffeners for both flat and shallow-curved plates.[7-17] Discussions of effective width and postbuckling strength of plates as well as summaries of the most commonly used effective-width criteria appear in Refs. 18 and 19. However, all referenced data are based on either linear-elastic analysis or the fitting of relations to empirical results, both of which are questionable procedures for understanding elastoplastic postbuckling behavior to the crippling-load level of nonlinear materials such as conventional metals and advanced composites. No widely accepted, theoretically derived criterion, either government-agency or industry-generated, exists for determining the effective width of buckled skin in conventional metals and composite flat and shallow-curved plates. Nevertheless, it has been demonstrated that accurate predictions of both crippling and effective width are achievable by theoretical elastoplastic analysis, at least for flat and shallow-curved metal plates[20,21] and flat composite plates.[22,23]

Initial analysis of the postbuckling behavior of linear-elastic, isotropic shallow-curved plates can be traced to Levy.[24] Subsequent contributions of note are surveyed by Yoo.[21] In all instances, the results are restricted to isotropic plates which operate in the linear-elastic range. Materially nonlinear postbuckling of both flat and curved, conventional and composite plates has been investigated by Mayers et al. over a period spanning several decades.[20-28] The results, particularly those which have been correlated to the applicable and available experimental data reported in Refs. 29-37, indicate the accurately predictable load-carrying capability of postbuckled plates in the elastoplastic range and the remarkable similarity between the behavior of conventional metal and advanced composite configurations through buckling, postbuckling, and crippling. The most recent research, that of Arnold, the details of which are reported in Ref. 38 and summarized by Arnold and Mayers in Ref. 23, when combined with the study by Yoo,[21] provides the mechanism for investigating herein the compressive buckling, postbuckling, and crippling of shallow-curved composite panels with stiffeners supplying any degree of torsional restraint along sheet-stringer attachment lines.

Results for both conventional metal and composite shallow-curved plates are presented. The composite plate model is sufficiently general to include the conventional metal plate as a special case. Thus, the qualitative results of Yoo[21] are readily recovered; the original quantitative results are closely verified in general but improved in some instances by the inclusion of relatively more stringent convergence criteria. Since load-shortening curves are produced for the initial-buckling-to-crippling range, a readily available by-product of the computational process is the effective-width history of the buckled skin throughout the loading process. The effective width is least at crippling and, hence, the use of effective-width estimates made on the basis of linear-elastic analysis are unconservative. As a result, stiffened panels designed by the minimum-weight procedure can be expected to fail in test sooner than predicted, even in the absence of local-buckling-mode interaction precipitated by invariably present initial imperfections, including pre-buckling-process nonlinearities. Indeed, the realism of the "minimum-weight" approach has been questioned by Koiter[39] and others.

In summary, the present work, an extension of earlier work undertaken by Yoo[21] and Arnold and Mayers,[23] unifies the treatment of the buckling, postbuckling, and crippling of edge-stiffened conventional metal and laminated composite plates of either flat or shallow-curved geometry. In addition, through correlation with experimental results available in the literature, the theory and analysis procedure are justified to the extent that a tool can be considered to exist for use in the preliminary design process. Of importance is the fact that costly and time-consuming effort inherent in the design and test of complex structures/materials combinations, specifically arbitrarily angle-plied and stacked composites, can be reduced to a computational exercise, with a requirement to test only a very limited number of specimens for verification.

With the structural mechanics well established, solutions for loading in both shear and combined shear and compression are within reach.

Theory

Problem Statement and Basic Assumptions

The problem being studied is the buckling, postbuckling, and crippling of shallow-curved composite plates with edge stiffeners. A typical example of this basic structural element is shown in Fig. 1 for either metal or composite-material construction. For purpose of demonstrating a solution, the theoretical model is restricted to edge stiffening which permits only extensional and torsional deformation of the stiffeners to take place.

The primary objective of this effort is to investigate both the effects of curvature in the plate and torsional and axial rigidity of the edge stiffeners on the elastic buckling and elastoplastic postbuckling of the plate. The model is valid up to a point at which the maximum strength of the plate is reached, whereupon the crippling of the plate governs the ultimate failure load.

The load is assumed to be one corresponding to a uniform end shortening. Loaded edges are assumed to be simply supported; the unloaded edges are constrained to remain straight although they are free to translate in the x-y surface.

The plate consists of N homogeneous and materially nonlinear anisotropic laminae with each lamina having thickness t_{fm_k}. Each element of a lamina midsurface can undergo three translations, two in-plane displacements, u_k and v_k ($k=1,2,\ldots,N$), and a lateral displacement, w, which is common to all laminae. The stresses σ_{x_k}, σ_{y_k}, and τ_{xy_k} are assumed constant through the thickness of each laminae. The bending stiffness of an individual lamina is assumed negligible compared wo that of the laminate; i.e., lamina are assumed to behave as membranes. Consequently, transverse shear effects are accommodated by permitting relative movement between the median planes of adjacent laminae. The matrix material between adjacent laminae is assumed to carry all of the transverse shear in the x-y and z-x planes. The normal stress (σ_z) is taken to be negligible in comparison with the other interlaminar stresses (τ_{yz}, τ_{zx}) for the composite plates considered herein; namely, those that buckle in the linear-elastic range and become nonlinear elastic in the postbuckling range. This particular model for the laminated plate was advanced by Anderson and Mayers[22] in an earlier work concerned with the application of a modified version of Reissner's variational principle to the analysis of nonlinear composite-material plates undergoing postbuckling.

In an earlier effort by Yoo,[21] a model for isotropic, shallow-curved plates was developed and applied to the prediction of plate crippling under axial compression. This model provides a convenient reference point for the laminated model used in the present investigation. Yoo's model uses a two-element, isotropic, rigid core sandwich-plate model first introduced by Mayers and Budiansky[25] for analyzing the elastoplastic postbuckling behavior of isotropic flat plates. Transverse shear effects are automatically excluded from the work of Yoo, inasmuch as the model uses the Kirchoff-Love hypothesis in the derivation of the strain-displacement relations.

The stiffeners are assumed to be sturdy in that local instability of stiffeners is not considered prior to crippling of the plate. Furthermore, only the torsional and extensional stiffnesses of the stiffeners are assumed to be present. As a consequence, the cross-sectional shape of the stiffener remains unchanged throughout the loading process. Also, mutual rotation of the stiffener and plate element is assumed to occur along lines of attachment. Stiffener eccentricity and shear-lag effects are neglected. For the composite stiffener, classical lamination theory is used to calculate the appropriate extensional and torsional stiffnesses. A complete presentation of the underlying theory can be found in Refs. 21-23 wherein the Reissner Variational Theorem[40] is used.

Method of Solution

The modified Reissner functional developed in Refs. 20-23 can be expressed in vector-matrix notation in which the variational quantities of displacement and stress are, in turn, expressed as a series of suitable distribution functions, each term multipled by an amplitude of unknown magnitude. The mechanics of this approach are discussed in Ref. 41. When the modified Reissner functional is expressed in vector-matrix form and the first variation is performed, a set of ten simultaneous, nonlinear, integral equations is obtained. The solution of these equations for a specific set of assumed displacement and stress spatial distributional functions is made possible by applying the Newton-Raphson iterative-solution technique. By expanding the set of simultaneous equations in a Taylor series, it is possible to obtain another set of ten simultaneous, linear, integral vector-matrix equations which contain the final equations of the generalized solution procedure. For this particular problem, the following displacement and stress functions are chosen:

$$u=-\delta x+\left(\frac{z}{h}\right)\left\{e_{21}\cos\frac{m\pi x}{L}\cos\frac{n\pi y}{b}+e_{22}\cos\frac{pm\pi x}{L}\times\cos\frac{qn\pi y}{b}+e_{23}\cos\frac{m\pi x}{L}\left(1+\cos\frac{2n\pi y}{b}\right)\right\} \tag{1}$$

$$v=v_0 y+\left(\frac{z}{h}\right)\left\{f_{21}\sin\frac{m\pi x}{L}\sin\frac{n\pi y}{b}+f_{22}\sin\frac{pm\pi x}{L}\sin\frac{qn\pi y}{b}+f_{23}\sin\frac{n\pi y}{b}+f_{24}\sin\frac{m\pi x}{L}\sin\frac{2n\pi y}{b}\right)\right\} \tag{2}$$

$$w=g_1\cos\frac{n\pi y}{b}+g_2\sin\frac{m\pi x}{L}\cos\frac{n\pi y}{b}+g_3\sin\frac{m\pi x}{L}\left(1+\cos\frac{2n\pi y}{b}\right)+g_4\sin\frac{pm\pi x}{L}\cos\frac{qn\pi y}{b} \tag{3}$$

$$\sigma_x=h_{111}+h_{112}\left(\frac{2y}{nb}\right)^2+h_{113}\left(\frac{2y}{nb}\right)^4+\left[\left(\frac{2mx}{L}\right)^2-\frac{1}{2}\left(\frac{2mx}{L}\right)^4+2\alpha\left(3\left(\frac{2mx}{L}\right)-\left(\frac{2mx}{L}\right)^3\right)\right]\times\left[h_{114}\left(1-3\left(\frac{2y}{nb}\right)^2\right)+h_{115}\left(\left(\frac{2y}{nb}\right)^4-\frac{3}{5}\left(\frac{2y}{nb}\right)^2\right)\right]+\frac{z}{h}\left\{\sin\frac{m\pi x}{L}\left[h_{121}+h_{122}\cos\frac{n\pi y}{b}+h_{123}\cos\frac{2n\pi y}{b}\right]+h_{124}\cos\frac{n\pi y}{b}+h_{125}\sin\frac{pm\pi x}{L}\cos\frac{qn\pi y}{b}\right\} \tag{4}$$

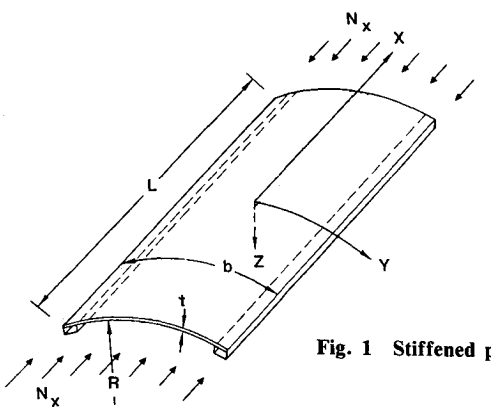

Fig. 1 Stiffened panel geometry.

$$\sigma_y = \left(\frac{mb}{L}\right)^2 \left\{ h_{211}\left(\left(\frac{2mx}{L}\right)^2 - \frac{1}{3} + 2\alpha\left(\frac{2mx}{L}\right)\right) + h_{212}\left(\left(\frac{2mx}{L}\right)^4 - \frac{1}{5} + 4\alpha\left(\left(\frac{2mx}{L}\right)^3 - 2\left(\frac{2mx}{L}\right)\right)\right) + h_{213}\left(\left(\frac{2mx}{L}\right)^6 - \frac{1}{7} + 2\alpha\left(\frac{2mx}{L}\right)\left(3\left(\frac{2mx}{L}\right)^4 - 20\left(\frac{2mx}{L}\right)^2 + 48\right)\right) - 3\left(\left(\frac{2mx}{L}\right)^2 - \frac{1}{3} + 2\alpha\left(\frac{2mx}{L}\right)\right) \times \left[h_{114}\left(\frac{2y}{nb}\right)^2 \left(1 - \frac{1}{2}\left(\frac{2y}{nb}\right)^2\right) + \frac{1}{15} h_{115}\left(\frac{2y}{nb}\right)^4 \times \left(\left(\frac{2y}{nb}\right)^2 - \frac{3}{2}\right)\right]\right\} + \left(\frac{z}{h}\right)\left\{ \sin\frac{m\pi x}{L}\left[h_{221} + h_{222}\cos\frac{n\pi y}{b} + h_{223}\cos\frac{2n\pi y}{b}\right] + h_{224}\cos\frac{n\pi y}{b} + h_{225}\sin\frac{pm\pi x}{L}\cos\frac{qn\pi y}{b}\right\} \tag{5}$$

$$\tau_{xy} = \left(\frac{mb}{L}\right)\left\{ 2\left(\left(\frac{2mx}{L}\right)^3 - \left(\frac{2mx}{L}\right) + 3\alpha\left(\left(\frac{2mx}{L}\right)^2 - 1\right)\right) \times \left(h_{114}\left(\frac{2y}{nb}\right)\left(1 - \left(\frac{2y}{nb}\right)^2\right) + \frac{1}{5} h_{115}\left(\frac{2y}{nb}\right)^3 \times \left(\left(\frac{2y}{nb}\right)^2 - 1\right)\right)\right\} + \left(\frac{z}{h}\right)\left\{ \cos\frac{m\pi x}{L}\left[h_{321}\sin\frac{n\pi y}{b} + h_{322}\sin\frac{2n\pi y}{b}\right] + h_{323}\cos\frac{pm\pi x}{L}\sin\frac{qn\pi y}{b}\right\} \tag{6}$$

$$\tau_{yz} = \left(\frac{z}{h}\right)\left\{ b_{11}\cos\frac{m\pi x}{L}\cos\frac{n\pi y}{b} + b_{12}\cos\frac{pm\pi x}{L}\cos\frac{qn\pi y}{b} + b_{13}\cos\frac{m\pi x}{L}\left(1 + \cos\frac{2n\pi y}{b}\right)\right\} \tag{7}$$

$$\tau_{zx} = \left(\frac{z}{h}\right)\left\{ a_{11}\sin\frac{m\pi x}{L}\sin\frac{n\pi y}{b} + a_{12}\sin\frac{pm\pi x}{L}\sin\frac{qn\pi y}{b} + a_{13}\sin\frac{n\pi y}{b} + a_{14}\sin\frac{m\pi x}{L}\sin\frac{2n\pi y}{b}\right\} \tag{8}$$

$$\sigma_s = h_{41} \tag{9}$$

$$\tau_s = h_{61}(mb/L)\cos(m\pi x/L) \tag{10}$$

where

$\alpha = 0$ for $Z \to 0$ (flat plate; shallow-curved square plate)

and

$$\alpha = 1 \quad \text{for} \quad Z \neq 0 \quad \text{(shallow-curved long plate)} \tag{11}$$

Functions for the out-of-plane displacement, the plate membrane and bending stresses, and the stiffener axial and torsional stresses are obtained from Yoo.[21] Because the current formulation is based on a laminae summation procedure, additional functions for the bending displacements, u, and v, and the transverse shear stresses, τ_{zx} and τ_{yz}, have been added. The totality of functions presented in Eqs. (1-10) represents the assumed solutions for composite, shallow-curved stiffened panels.

The linear membrane-displacement functions used in Ref. 21 are adopted for the present analysis. The underlying reason for this choice of functions is that the variational process becomes independent of u and v_0; the former because the unit end shortening e is a prescribed quantity and possesses no variation, and the latter because the arbitrary state of stress admissible in the application of the Reissner principle can be selected to render the variational process independent of v_0.

The g_2 and g_3 terms in the lateral-displacement function represent the buckling mode shapes of thin plates with either simply supported or clamped unloaded edges, respectively. The g_1 term is included to accommodate the curvature effect in the initial postbuckling range of long curved plates; it is eliminated in the case of the square curved-plate analysis since the term then violates the geometric boundary condition of vanishing lateral displacement, w, at the loaded edges. The g_4 term represents waveform changes due to advanced postbuckling. In the present analysis, $p = 1$ and $q = 3$ for long plates along with $p = 3$ and $q = 1$ for square plates are used since these combinations, along with the g_2 term, prove to provie lower postbuckling strengths (or strain energies) for given unit end-shortening values than any other combinations of the $p = 1, 3$ and $q = 1, 3$ harmonics.

It is to be noted that in the establishment of linear-elastic approximate solutions of the von Kármán-Donnell curved plate equations, the usual procedure is to satisfy the membrane equilibrium equations through the introduction of an Airy-type stress function and establish the membrane-stress distributions as a function of the assumed lateral-displacement waveform using the condition of compatibility. Approximate satisfaction of the remaining equilibrium equations is then obtained from application of the potential energy principle. In the present nonlinear-elastic study, which is founded upon use of the von Kármán-Donnell plate theory extended to include transverse shear effects and the Reissner variational principle, the membrane equilibrium equations are normally satisfied approximately in the variational process. Here, however, no free parameters relating to membrane displacements have been permitted to appear in the variational equation, thus requiring that the membrane equilibrium equations be satisfied externally. This procedure is justified on the basis that the constitutive relations are being satisfied along with the lateral equilibrium equation through the variation of both arbitrary-displacement and stress states; thus, no significant penalty accrues by making the variational process independent of arbitrary membrane displacement parameters as long as the assumed stress distrbutions are sufficiently general in character relative to the assumed displacement distributions.

In the assumed membrane displacement distribution functions, Eqs. (1-3), the requirement that a flat or shallow-curved square plate have zero shear stress on the loaded ends leads to the specification of $\alpha = 0$.

The bending and twisting stress distributions are selected in the form of the curvatures generated by the assumed lateral-displacement function, w, with free parameters introduced to establish bending stress magnitudes. For square plates, h_{124} and h_{224} are taken to be zero.

The bending displacement terms of Eqs. (1-3) and the transverse shear-stress terms of Eqs. (7) and (8) are chosen to be compatible with the out-of-plane displacement, w; this is consistent with the laminae summation model of the present theory. These additional terms, not present in Yoo's isotropic plate model, are required to effect a properly coupled laminated composite model.

Results and Discussion

Linear-Elastic Buckling and Postbuckling of Isotropic Plates

To place the present study of elastic buckling and elastoplastic postbuckling of uniaxially compressed, composite

shallow-curved plates with unloaded edges rotationally restrained by stiffeners in proper perspective, the work of Yoo[21] on edge-stiffened conventional plates, a special case of the analysis herein, is reviewed. Thus, it is appropriate first to reduce the present model to the special case (isotropic properties and transverse shear effects neglected) and compare results to those obtained for both flat and shallow-curved isotropic plates by Yoo and preceding investigators.

Long Plates

In Fig. 2, uniaxial compression buckling loads, normalized with respect to the buckling load of the corresponding simply supported flat plate, are shown as a function of the curvature parameter Z for several values of the torsional-stiffness parameter G_sJ_s/Db associated with the edge stiffening. The lowermost solid curve ($Z=0$) represents the solution first obtained by Leggett[42] for long, simply supported plates with unloaded edges held straight in the x-y plane. It is reproduced exactly by the initial buckling solution of the present special-case analysis, which serves to further converge some of the numerical results of Yoo.[21] The earlier solutions by Timoshenko[8] for plates with unloaded edges free to distort in the tangent plane are shown by the dashed curve. The uppermost curve represents an edge-stiffened plate with stiffener torsional rigidity essentially equivalent to full clamping, since it is indistinguishable from the results obtained originally by Leggett for fully clamped edges. The intermediate solid curve represents torsional restraint of a magnitude associated with practically proportioned stiffening. Yoo[21] has shown that the transition from essentially pinned edges to essentially fully clamped edges takes place in the range $0.1<G_sJ_s/Db<10$. No previous solutions are known to exist for this case of finite torsional restraint and unloaded edges constrained to remain straight. Stowell[43] (curved plates) and Wittrick and Bodley[44] (flat plates) have presented solutions in this range for torsionally restrained plates with unloaded edges free to distort in the plane. As shown by Yoo, Stowell's results for the weaker membrane-displacement boundary conditions fall as much as 20% below those of the straight-edged plate, whereas Wittrick and Bodley's results are reproduced almost exactly. For flat isotropic plates, with transverse shear effects neglected, buckling loads are independent of membrane displacements in general. It is shown also by Yoo that although increases in curvature and torsional restraint lead to increases in the buckling load ratio N/N_{cr}, they act more and more to equalize buckle aspect ratio L/mb in the vicinity of 0.5 as the shallow-curved plate upper limit of $Z\approx 12$ is approached.

In Figs. 3 and 4, postbuckling results produced by the present analysis, for which Yoo's work represents a special case, are shown for shallow-curved plates with $Z=0$, 5, and 10, $G_sJ_s/Db=0$ (essentially simply supported) and $G_sJ_s/Db=10^4$ (essentially clamped), $A_s/bt=0.5$, and $b/t=60$. The initial postbuckling slope for $Z=0$, $G_sJ_s/Db=0$ is 0.5, as it should be for the simply supported flat plate with straight unloaded edges.[45] Pope[46] has studied the postbuckling of shallow-curved plates with straight, unloaded edges and either vanishing or infinite torsional restraint; however, in each of these extreme cases, only the load-shortening curve for the flat-plate case is shown since it provides the lower-bound approach by Pope's curved-plate results. Beyond the early postbuckling range, Pope's results become increasingly more unconservative due to the constraining assumption that the buckle waveform at initial buckling persists throughout the postbuckling range, thereby precluding appropriate redistribution of stresses.

Square Plates

Unlike flat isotropic plates of square planform, which possess a unique linear-elastic postbuckling behavior, corresponding shallow-curved plates evidence two possible postbuckling branches beyond initial buckling—one representing

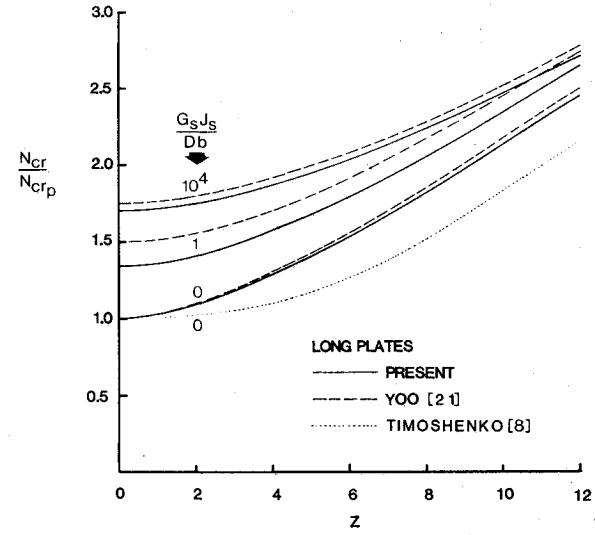

Fig. 2 Effects of curvature and unloaded-edges boundary condition on compressive buckling load of long plates.

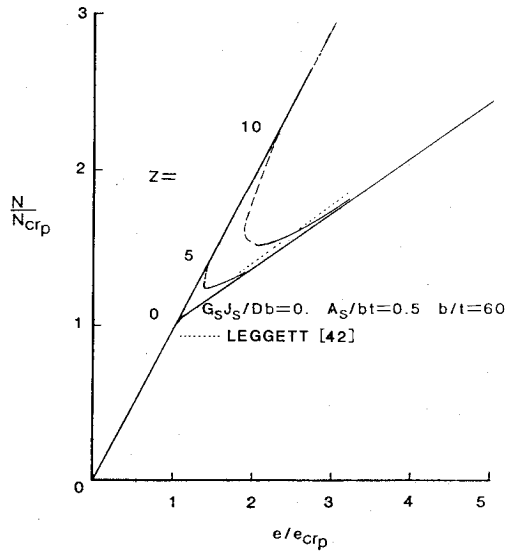

Fig. 3 Linear-elastic load-shortening curves of long, simply supported shallow-curved plates.

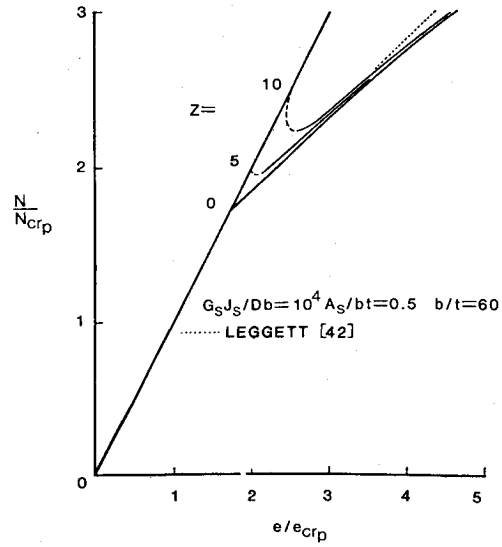

Fig. 4 Linear-elastic load-shortening curves of long, essentially clamped shallow-curved plates.

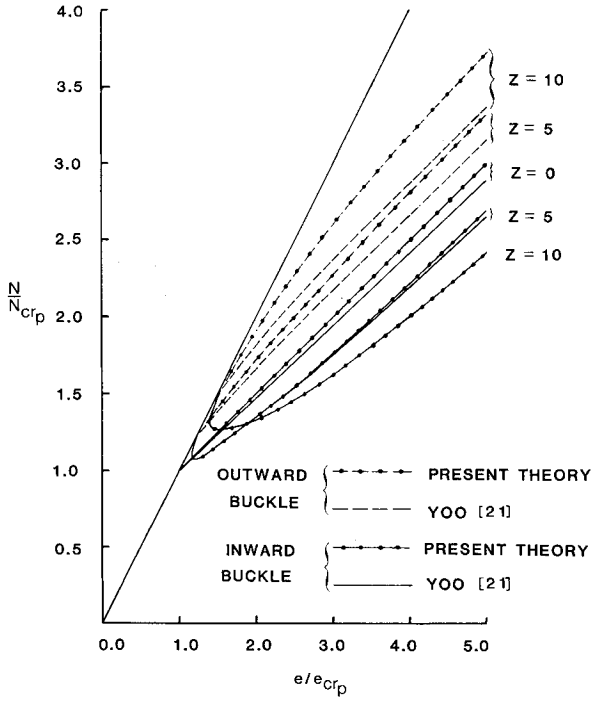

Fig. 5 Load-shortening curves of simply supported square shallow-curved plates.

buckling inward and the other buckling outward. The effect on the buckling-load parameter N/N_{cr} as a function of end-shortening ratio e/e_{cr} is shown in Fig. 5 for $Z=0$, 5, and 10. Here an obvious computational discrepancy appears between the results of Yoo[21] and those of the current analysis, the basic equations and trial functions of which, specialized appropriately to the isotropic medium, reproduce those appearing in Ref. 21. The discrepancy is limited basically to the case of outward buckling, a phenomenon which, in the absence of initial imperfections, is unlikely to occur based on energy considerations: the discrepancy becomes prominent (about 10% maximum, for the range shown) only for the $Z\rightarrow 10$ plates. It has been observed that more rapid convergence of solutions occurs for square plates with inward buckles; thus, Yoo's postbuckling curves for shallow-curved plates deforming in the outward mode must be deemed not quite converged. In view of the 28 nonlinear equations being solved simultaneously in the isotropic case, the judgment appears reasonable.

For square, shallow-curved plates with unloaded edges held straight during the buckling and postbuckling process, Levy[24] has presented results restricted to the inward deformation mode for $Z=0$, 5, and 10. As shown by Yoo,[21] excellent agreement is obtained in the range $0<e/e_{cr}<3$, except for a growing discrepancy in the $Z=10$ case commencing at an end-shortening parameter ratio of about 1.4. In the present study this discrepancy has been removed. It is to be noted that Levy introduces six combinations of biaxial harmonics to describe the postbuckling waveform; in Ref. 21, as well as in the present analysis, only two combinations are used for isotropic square plates since stresses are taken independently when using Reissner's variational principle. Volmir,[48] Tamate and Sekine,[49] and Hsueh and Chajes[50] have investigated the postbuckling of shallow-curved square plates with unloaded edges not constrained to remain straight. The latter two studies yield results reflecting lower postbuckling strengths, whereas Volmir's results, because of greater and more influential constraint placed on membrane displacements at the plate corners, yield greater postbuckling strengths than those given by either Yoo or the present analysis.

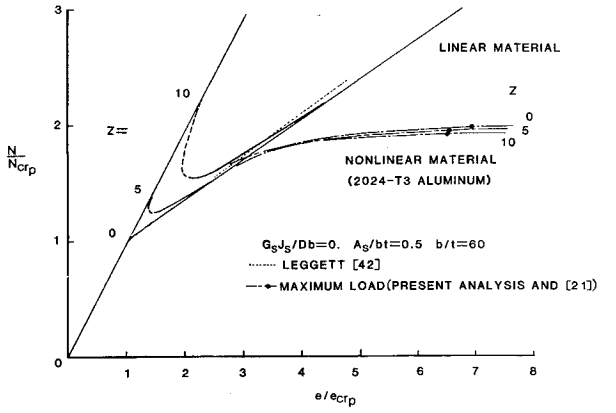

Fig. 6 Elastoplastic load-shortening curves of long, simply-supported 2024-T3 aluminum shallow-curved plates.

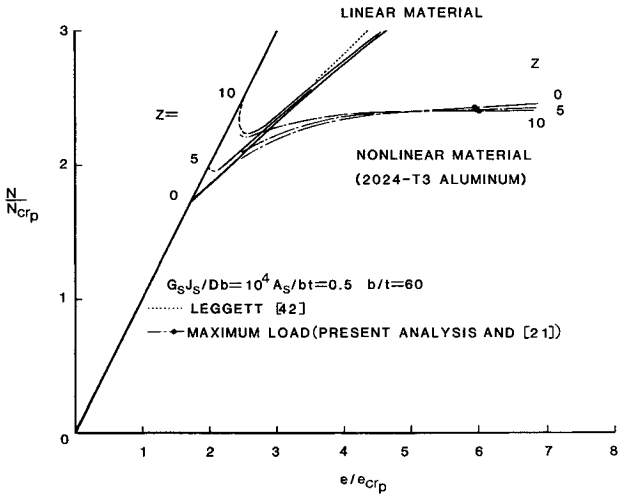

Fig. 7 Elastoplastic load-shortening curves of long, essentially clamped 2024-T3 aluminum shallow-curved plates.

Nonlinear Elastic Postbuckling and Crippling of Isotropic Plates

For the special case of isotropic properties, the present analysis has been used to develop elastoplastic load-shortening curves, Figs. 6 and 7, for the shallow-curved plate parameters specified in Figs. 3 and 4 and the 2024-T3 material stress-strain curve appearing in Fig. 8. The results are given in replots of Figs. 3 and 4 to illustrate the significant difference in behavior predicted by nonlinear-elastic as opposed to linear-elastic plate theory and analysis. Most important is the fact that linear-elastic analysis, no matter the degree of accuracy of the trial functions assumed in the solution procedure, cannot predict a crippling (maximum) load. In both figures, the load maxima of the current solutions are clearly evident. Such maxima have been obtained first by Mayers and Nelson[20] in achieving close correlation with experimental results reported by Stein[31] on crippling of a 2024-T3 flat aluminum plate with unloaded edges carefully constrained to remain straight; in the work of Yoo[21] on shallow-curved plates, Mayers and Nelson's results are closely reproduced for the limiting case $Z=0$ and $G_sJ_s/Db=0$. A review of Fig. 2 suggests that increasing the rise of a curved plate and the torsional rigidity of the edge stiffeners simply to raise the initial or bifurcation buckling load cannot be expected to produce comparable increases in the crippling load. That is, increases in Z imply greater imperfection sensitivity and, hence, nonbifurcation buckling at reduced load levels; increases in the degree of torsional restraint lead to greater average loads (or stresses) during postbuckling and,

as a result, greater penalties for nonlinear material effects (see Ref. 27). In any event, except in the vicinity of buckling, there is little to distinguish crippling loads of shallow-curved plates with either vanishing or essentially unbounded torsional restraint from the crippling loads of the corresponding flat plates. This relationship between shallow-curved and flat plates was noted first by Levy.[47] In other words, the effect of curvature is manifested only in the region of bifurcation buckling; the curvature effect would be further diminished when, in the presence of initial imperfections, nonbifurcation buckling occurs.

With load-shortening curves predictable through crippling, accurate estimates of plate effective-width for both stiffened and unstiffened plates are readily obtainable. Extensive treatment of effective-width prediction and comparison with a myriad of existing effective-width formulas for square and rectangular, flat and shallow-curved isotropic plates, developed over a period of some 50 years on the basis of linear-elastic theory by von Kármán et al.,[7] Koiter,[39] Levy,[47] and others, are presented by Yoo.[21] The study demonstrates clearly that rigorously speaking, only the results of a nonlinear-elastic plate postbuckling analysis can be valid for predicting effective width and crippling as well as correlating theory and analysis with observation. Effective width, which is generally defined as the ratio $b/b_e = N_{av}/Et = \sigma_{av}/E$ in linear-elastic analysis, must be obtained as $\sigma_{av}/\sigma_{edge}$ in analyses wherein nonlinearity of the relationship between stresses and strains cannot be discounted. In addition, Yoo's results for stiffened plates validate Gerard's[18] semi-empirical design curve parameters for stiffened plates and explain the major reason for the ±10% scatter in Gerard's correlation with a myriad of experiments.

To illustrate the accuracy of theoretical prediction vs experiments in the case of conventional plates, the present model is reduced to the special-case model of Yoo[21] and load-shortening curves are obtained for the 2024-T3 aluminum material stress-strain curve of Fig. 8 and plate geometric parameters shown in Fig. 9. The experimental load-shortening curves, corresponding to the specific additional stress-strain curves in Fig. 9, are taken from Botman and Besseling.[29] The experimental fixture has been designed to provide unloaded-edge boundary conditions in closely corresponding to straight unloaded edges, the condition specified in the analysis. The discrete points are the results of numerical solution and indicate that both postbuckling stiffness during loading and average load (or stress) at crippling can be accurately predicted. The plate effective width at any point up to crippling is the ratio of the average load (or stress) to the average load (stress) the plate would carry if it were to remain linear-elastic and unbuckled. Both effective width and postbuckling stiffness (reduced effective width) during loading are increasingly underestimated by linear-elastic analyses.

Buckling, Postbuckling, and Crippling of Composite Plates

The present nonlinear-elastic postbuckling analysis, which either reproduces or improves the stiffened and unstiffened, flat and shallow-curved isotropic plate results of Yoo[21] and the unstiffened, flat composite plate results of Arnold and Mayers[23] is used to develop load-shortening curves (N/N_{cr} vs e/e_{cr}) for both a stiffened and an unstiffened shallow-curved plate of a typical composite material. The results are shown in Figs. 10 and 11 for plates of A-S/3501-5 graphite-epoxy arranged in a $(\pm 45°/0/90)_S$ layup. As in the case of conventional plates, the marked difference in linear-elastic vs nonlinear-elastic material behavior is evident. The parameters of the stiffened plate have been selected to represent a shallow-curved plate corresponding to a specimen proposed for testing.

It is remarked first that the buckling loads include transverse shear effects and the predicted crippling loads are based on application of the maximum-strain failure criterion justified in the study by Arnold and Mayers[23] through correlation of theoretical analysis prediction with the experimental results of Spier[33-37] for rectangular flat plates representing seven different layups of graphite-epoxy material. However, an experimental crippling load in the fiber-failure sense does appear in the literature for a shallow-curved plate. Thus, at this time, it is not possible to compare the present analysis crippling-load prediction to experiment. But, as illustrated earlier and attributable to Levy,[47] the postbuckling curve for a shallow-curved plate approaches that of the

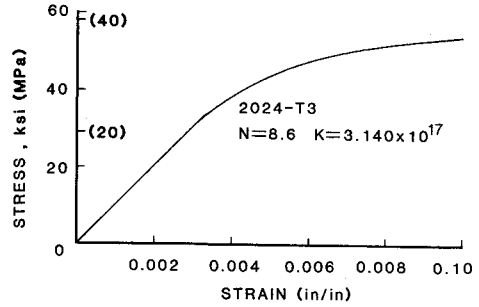

Fig. 8 Stress-strain curve for 2024-T3 aluminum.

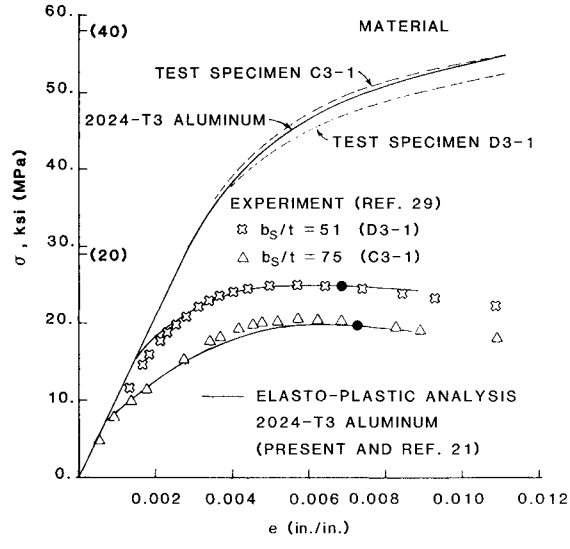

Fig. 9 Comparison of theory and experiment for crippling of simply supported flat plates in compression.

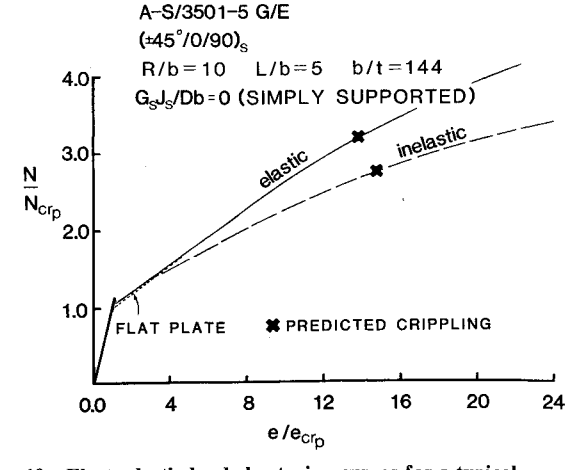

Fig. 10 Elastoplastic load-shortening curves for a typical composite stiffened plate with simply supported boundary conditions on unloaded edges.

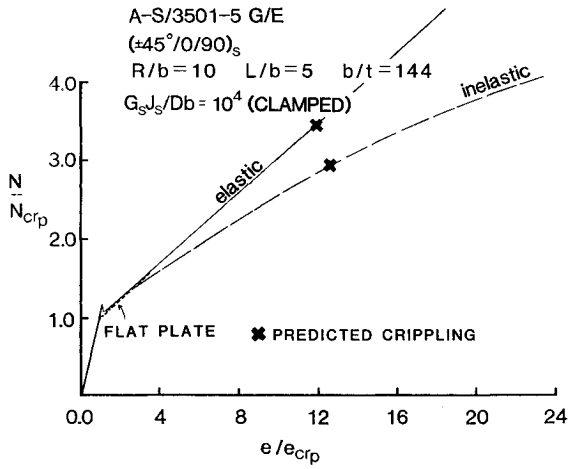

Fig. 11 Elastoplastic load-shortening curves for a typical composite stiffened plate with essentially clamped boundary conditions on unloaded edges.

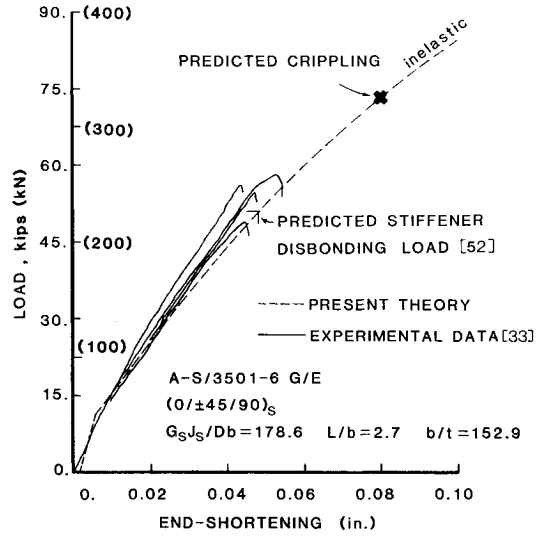

Fig. 12 Comparison of predicted and experimentally determined load-shortening curves for a stiffened panel in compression.

equivalent flat plate beyond the initial buckling region. Thus, based on the extremely high degree of success achieved by Arnold and Mayers in predicting crippling in composite flat-plate experiments, it would appear that the same trend and degree of accuracy in predicting fiber failure in the curved plate should apply. It is safe to conclude, then, that Figs. 10 and 11 provide the crippling (maximum) strengths of the given shallow-curved composite plates.

Stiffened composite plates with bonded stiffeners are subject to premature failure when bond integrity between plate and stiffener is lost. Test results exist for stiffened flat plates which reflect this failure mode.[51] The application of a disbond criterion developed by Arnold[52] and based on the present theory leads to the comparison of the experimental and predicted disbond-load levels shown on the load-shortening curves presented in Fig. 12. The agreement obtained can be considered a reliable indicator of the validity of the disbond criterion and stiffener model based upon the results to become available in Ref. 52. It is important to note that prevention of the disbonding phenomenon would lead to an increase in failure load of 25% or more in each of the four cases.

Concluding Remarks

Theory and analysis procedure applicable to buckling, postbuckling, and crippling in uniaxial compression of materially nonlinear, shallow-curved, laminated composite plates with edge stiffeners have been presented. The structural mechanics model developed represents extensions of earlier work on both flat and shallow-curved conventional plates with edge stiffeners and unstiffened flat composite plates. Although the earlier studies have achieved validity on the basis of close correlation of theory/analysis predictions with available experimental results, the dearth of test data on shallow-curved composite plates possessing sturdy but torsionally flexible stiffeners along plate unloaded edges prevents direct assessment of the accuracy of the results of the latest investigation. Nevertheless, since it is known that once buckling has occurred in both stiffened and unstiffened shallow-curved plates, the load-shortening curves approach closely the load-shortening curves of the corresponding flat plates. Pending the generation of appropriate test data, the crippling loads of curved composite plates can be predicted accurately by using results obtained for composite flat-plate counterparts.

Finally, although only uniaxial compression of shallow-curved composite plates has been treated, additional load cases such as shear and combined shear and compression are readily tractable to solution simply by introducing appropriate trial functions; the structural mechanics theoretical model and the solution technique remain unchanged. In general, then, the theory and analysis procedure provide a tool for the design process. In this respect, the costly and time-consuming effort inherent in the design and test of complex structures/materials combinations, specificially arbitrarily angle-plied and stacked composite plates, with characteristics consistent with the basic assumptions, can be reduced to a computational exercise, with a requirement to test only a very limited number of specimens for verification.

Appendix: Stiffener Theoretical Formulation

In addition to the theory and equations previously provided in Ref. 23, the following is required to complete the stiffened-panel formulation.

Strain-Displacement Equations

For the stiffener, the extensional and torsional strain-displacement relations are, respectively,

$$\epsilon_{s_{x_k}} = \frac{\partial u_k}{\partial x} + \frac{1}{2}\left(\frac{\partial w}{\partial x}\right)^2 \tag{A1}$$

$$\gamma_{s_k} = \rho \frac{\partial^2 w}{\partial x \partial y} \tag{A2}$$

where ρ is the distance from the plate middle surface to a point in the stiffener cross section; the origin of ρ is a point lying in a plane perpendicular to the plate middle surface and containing the plate-stiffener juncture line.

Constitutive Relations

The material model for the stiffener is defined as a "lumped" mass possessing a specified overall behavior which is presumably known from experimental testing. Thus,

$$\epsilon_s = \frac{\sigma_s}{E_s} + K_{s_\sigma}\left(\frac{\sigma_s}{E_s}\right)^{n_{s_\sigma}} \tag{A3}$$

$$\gamma_s = \frac{\tau_s}{G_s} + K_{s_\tau}\left(\frac{\tau_s}{G_s}\right)^{n_{s_\tau}} \tag{A4}$$

E_s is the axial elastic modulus of the stiffener, and K_{s_σ}, n_{s_σ}, K_{s_τ}, and n_{s_τ} are Ramberg-Osgood parameters for the stiffener.

Modified Reissner Functional

The energy associated with the stiffeners is given by

$$F_s''=F_{s_\sigma}''+F_{s_\tau}'' \tag{A5}$$

where

$$F_{s_\sigma}''=\int_V(\sigma_s\epsilon_s-F_{s_\sigma}')\mathrm{d}V \tag{A6}$$

and

$$F_{s_\tau}''=\int_V(\tau_s\gamma_s-F_{s_\tau}')\mathrm{d}V \tag{A7}$$

are the contributions from axial and torsional stresses, respectively. The stress-energy-density functions are

$$F_{s_\sigma}'=\frac{1}{2}\frac{\sigma_s^2}{E_s}+\frac{K_{s_\sigma}}{(n_{s_\sigma}+1)}\left(\frac{1}{E_s}\right)^{n_{s_\sigma}}(\epsilon_s)^{(n_{s_\sigma}+1)/2} \tag{A8}$$

$$F_{s_\tau}'=\frac{1}{2}\frac{\tau_s^2}{G_s}+\frac{K_{s_\tau}}{(n_{s_\tau}+1)}\left(\frac{1}{G_s}\right)^{n_{s_\tau}}(\tau_s)^{(n_{s_\tau}+1)/2} \tag{A9}$$

Thus, the total energy associated with the stiffener [Eq. (A5)] is added to that of the plate [Eq. (8) of Ref. 23.]

Acknowledgments

The first author extends his appreciation to the General Dynamics Convair Division for funding the composite mechanics portion of the research.

References

[1]Air Force Project Forecast, 1965.

[2]Hotz, R., "A New Materials Revolution," *Aviation Week & Space Technology,* Vol. 89, Sept. 1968, p. 11.

[3]Boeing Advanced Technology Forum, Boeing Aircraft Co., Seattle, WA, June 1981.

[4]Burke, E. C., "Light Metal Alloys and Metal-Matrix Composite Materials," Presented at the AIAA Annual Meeting, Baltimore, MD, April 1982.

[5]Bohon, H. L. and Davis, J. G. Jr., "Composites for Large Transports—Facing the Challenge," *Aerospace America*, June 1984, pp. 58-62.

[6]Wigotsky, V., "Lightweight Aluminum-Lithium Alloys Poised for Takeoff," *Aerospace America,* Vol. 22, June 1984, pp. 74-77.

[7]von Kármán, T., Sechler, E. E., and Donnell, L. H., "The Strength of Thin Plates in Compression," *Transactions of the American Society of Mechanical Engineers,* Vol. 54, No. 2, 1932, pp. 53-57.

[8]Timoshenko, S., *Theory of Elastic Stability,* McGraw-Hill Book Co., New York, 1936.

[9]Marguerre, K., "The Apparent Width of the Plate in Compression," NACA TM 833, 1937.

[10]Bengston, H. W., "Ship Plating Under Compression and Hydrostatic Pressure," *The Society of Naval Architects and Marine Engineers, Transactions,* Vol. 47, 1939, pp. 80-116.

[11]Levy, S., "Benind of Rectangular Plates with Large Deflections," NACA Rept. 737, 1942.

[12]Koiter, W. T., "De meedragende breedte bij groote overschrijding der knikspanning voor verschillende inklemming der plaatranden" ("The Effective Width at Loads far in Excess of the Critical Load for Various Boundary Conditions"), Nationaal Luchtvaartlaboratorium, Amsterdam, the Netherlands, NLL Rept. S. 287, 1943.

[13]Gerard, G., "Effective Width of Elastically Supported Flat Plates," *Journal of the Aeronautical Sciences,* Vol. 13, No. 10, 1946, pp. 518-524.

[14]Winter, G., "Strength of Thin Steel Compression Flanges," *Transactions of the American Society of Civil Engineers,* Vol. 112, 1947, pp. 527-576.

[15]Coan, J. M., "Large Deflection Theory for Plates with Small Initial Curvature Loaded in Edge Compression," *Journal of Applied Mechanics,* Vol. 18, No. 2, 1951, pp. 143-151.

[16]Argyris, J. H. and Dunne, P. C., *Handbook of Aeronautics, No. 1, Structural Principles and Data, Part 2: Structural Analysis,* 4th Ed., Pitman Publishing Corp., New York, 1952.

[17]Yamaki, N., "Postbuckling Behavior of Rectangular Plates with Small Initial Curvature Loaded in Edge Compression," *Journal of Applied Mechanics,* Vol. 26, No. 3, 1959, pp. 407-414.

[18]Gerard, G., "Handbook of Structural Stability, Part IV—Failure of Plates and Composite Elements," NACA TN 3784, 1957.

[19]Jombock, J. R. and Clark, J. W., "Postbuckling Behavior of Flat Plates," *Transactions of the American Society of Civil Engineers,* Vol. 127, Pt. II, 1962, pp. 227-243.

[20]Mayers, J. and Nelson, E., "Elastic and Maximum Strength Analyses of Postbuckled Rectangular Plates Based Upon Modified Versions of Reissner's Variational Principle," AIAA Paper 68-171, Jan. 1968; also, USAAVLABS Tech. Rept. 69-64, July 1970 (AD 872 821).

[21]Yoo, S. Y., "On Maximum Strength of Plates Under Axial Compression—Effects of Curvature and Edge-Stiffener Extensional and Torsional Rigidity," Ph.D. Dissertation, Stanford University, Stanford, CA, 1977.

[22]Anderson, R. E. and Mayers, J., "Effects of Non-linear Material Behavior on Postbuckling Stiffness of Laminated Composite Plates," AIAA Paper 79-1806, Aug. 1979.

[23]Arnold, R. R. and Mayers, J., "Buckling, Postbuckling, and Crippling of Materially Nonlinear Laminated Composite Plates," *International Journal of Solids and Structures,* Vol. 20, 1984, pp. 863-880.

[24]Levy, S., "Large-Deflection Theory of Curved Sheet," NACA TN 895, 1943.

[25]Mayers, J. and Budiansky, B., "Analysis of Behavior of Simply Supported Flat Plates Compressed Beyond the Buckling Load into the Plastic Range," NACA TN 3368, 1955.

[26]Mayers, J. and Wesenberg, D. L., "The Maximum Strength of Initially Imperfect Axially Compressed, Circular Cylindrical Shells," USAAVLABS Tech. Rept. 69-60, Aug. 1969 (AD 862 102).

[27]Wesenberg, D. L. and Mayers, J., "Failure Analysis of Initially Imperfect, Axially Compressed, Orthotropic, Sandwich and Eccentrically Stiffened, Circular Cylindrical Shells," USAAVLABS Tech. Rept. 69-68, Dec. 1969 (AD 866 199).

[28]Nimmer, R. P. and Mayers, J., "Limit Point Buckling Loads of Axially Compressed, Circular Cylindrical Shells," *Journal of Applied Mechanics,* Vol. 46, No. 2, 1979, pp. 386-392.

[29]Botman, M. and Besseling, J. F., "The Effective Width in the Plastic Range of Flat Plates Under Compression," National Luchtvaartlaboratorium, Amsterdam, the Netherlands, 1954, NLL Rept. S. 445.

[30]Peterson, J. P., Whitley, R. O., and Deaton, J. W., "Structural Behavior and Compressive Strength of Circular Cylinders with Longitudinal Stiffening," NASA TN D-1251, 1962.

[31]Stein, M., "Loads and Deformations of Buckled Rectangular Plates," NASA TR R-40, 1959.

[32]Gerard, G., "Handbook of Structural Stability, Part IV—Failure of Plates and Composite Elements," NACA TN 3784, 1957.

[33]Spier, E. E., "Local Buckling, Postbuckling, and Crippling Behavior of Graphite-Epoxy Short Thin Walled Compression Members," Department of the Navy, Naval Air Systems Command, Rept. NASC-N00019-80-C-0174, Washington, D. C. July 1981.

[34]Spier, E. E. and Klouman, F. L., "Postbuckling Behavior of Graphite/Epoxy Laminated Plates and Channels," Army Symposium on Solid Mechanics, Cape Cod, MA, Sept. 1976, pp. 62-78.

[35]Spier, E. E. and Klouman, F. L., "Empirical Crippling Analysis of Graphite/Epoxy Laminated Plates," Composite Materials: Testing and Design, 4th Conference ASTM STP-617, 1977, pp. 255-271.

[36]Spier, E. E., "On Experimental Versus Theoretical Incipient Buckling of Narrow Graphite/Epoxy Laminated Plates," AIAA Paper 80-0686, 1980.

[37]Spier, E. E., "Stability of Graphite/Epoxy Structures with Arbitrary Symmetrical Laminates," *Experimental Mechanics,* Vol. 18, No. 11, Nov. 1978, pp. 401-498.

[38]Arnold, R. R., "Buckling, Postbuckling, and Crippling of Materially Nonlinear Laminated Composite Plates," Ph.D. Dissertation, Stanford University, Stanford, CA, 1983.

[39]Koiter, W. T., "De meedragende breedte bij groote overschrijding der knikspanning voor verschillende inklemmingder plaatranden," ("The Effective Width at Loads Far in Excess of the Critical Load for Various Boundary Conditions,") National Luchtvaartlaboratorium, Amsterdam, the Netherlands, NLL Rept. S. 287, 1943.

[40]Reissner, E., "On a Variational Theorem in Elasticity," *Journal of Mathematics and Physics,* Vol. XXIV, No. 2, July 1950, pp. 90-95.

[41]Anderson, R. E., "A Variational Theorem for Laminated Composite Plates of Nonlinear Materials and Application to Postbuckling," Ph.D. Dissertation, Stanford University, Stanford, CA, 1979.
[42]Leggett, D. M. A., "The Buckling of a Long Curved Panel Under Axial Compression," ARC R&M 1899, 1942.
[43]Stowell, E. Z., "Critical Compressive Stress for Curved Sheet Supported Along Edges and Elastically Restrained Against Rotation Along the Unloaded Edges," NACA Restricted Bulletin 3I07, 1943.
[44]Wittrick, W. H. and Bodley, W. E., "Compressive Buckling of Infinite Strips with Elastically Restrained Edges," *The Aeronautical Quarterly,* Vol. XIV, May 1963, pp. 158-162.
[45]Hu, P. C., Lundquist, E. E., and Batdorf, "Effect of Small Deviations from Flatness on Effective Width and Buckling of Plates in Compression," NACA TN 1124, Sept. 1946.
[46]Pope, G. G., "On the Axial Compression of Long, Slightly Curved Panels," ARC R&M 3392, 1963.
[47]Levy, S., "Large-Deflection Theory of Curved Sheet," NACA TN 895, 1943.
[48]Volmir, A. S., "Flexible Plates and Shells," Moscow, 1956. English translation: AFFDL-TR-66-216, 1967.
[49]Tamate, O. and Sekine, H., "Postbuckling Behavior of Thin Curved Panels Under Axial Compression," *Bulletin of ASME,* Vol. 12, No. 51, 1969, pp. 415-420.
[50]Hsueh, P. S. and Chajes, A., "Buckling of Axially Loaded Cylindrical Panels," *Journal of the Engineering Mechanics Division, Proceedings of the American Society of Civil Engineers,* Vol. 97, No. EM3, 1971, pp. 919-933.
[51]Agarwal, B. L., "Postbuckling Behavior of Hat Stiffened Flat and Curved Composite Compression Panels," Department of the Navy, Naval Air Systems Command, Washington, D. C., Rept. NOR 81-187, Oct. 1981.
[52]Arnold, R. R., "Disbond Criterion for Postbuckled Composite Panels," Unpublished.